Thin-Walled Structures **18** (1994) 117–131

A Phenomenological Design Equation for FRP Columns with Interaction between Local and Global Buckling

Ever Barbero & John Tomblin

Mechanical and Aerospace Engineering, Constructed Facilities Center, West Virginia University, Morgantown, WV 26506-6101, USA

(Received 15 June 1992; revised version received 7 December 1992; accepted 15 March 1993)

ABSTRACT

A design equation for fiber reinforced plastic columns is presented in this paper, based on the interaction between local (flange) and global (Euler) buckling observed during testing of the FRP columns included in this investigation. An existing interaction equation is adapted to account for the modes of failure observed in columns made of fiber reinforced composite materials. Experimental data generated during this investigation are presented and used to validate the interaction equation and to obtain the interaction constant. A slenderness ratio is proposed and used to present a plot of buckling for all sections and column lengths (short, long, and intermediate). An expression for the optimum column length to be used in the experimental determination of the interaction constant is proposed.

1 INTRODUCTION

Pultruded composite beams and columns are being used for civil engineering structural applications[1] and aerospace applications.[2] Composite materials have many advantages over conventional materials (steel, concrete, wood, aluminum, etc.), such as light weight and high corrosion resistance. Mass production of composite structural members (e.g. by pultrusion) makes composite materials cost-competitive with conventional ones.

In the pultrusion process, fibers impregnated with a polymer resin are

Thin-Walled Structures 0263-8231/94/$07·00

pulled through a heated die that provides the shape of the cross-section to the final product. Pultrusion is a continuous process for manufacturing prismatic sections of virtually any shape.[3] Other mass-production techniques like automatic tape layout can also be used to produce prismatic sections.

Pultruded structural members have open or closed thin-walled cross-sections. For long composite columns, global (Euler) buckling is expected to occur before any other instability failure. The buckling equation has to account for the anisotropic nature of the material. Theoretical predictions correlate well with experimental data for long columns.[4] For short columns, local buckling occurs first, leading either to large deflections and finally to overall buckling, or to material degradation due to large deflections (crippling). Because of the large elongation of failure allowed by both the fibers and the resin, the composite material remains linearly elastic for large deflections and strains, unlike conventional materials that yield (steel) or crack (concrete) for moderate strains. Therefore, buckling is the governing failure for this type of cross-section and the critical buckling load is directly related to the load carrying capacity of the member. Theoretical predictions for short column buckling taking into account the anisotropy of the material correlate well with experimental observations.[5–7]

The experimental data for short and long column buckling[4–7] suggest the existence of an intermediate-column region where the critical loads are lower than the predictions of both local and global buckling theories. Since fiber reinforced plastics (FRPs) remain linearly elastic for large values of strain, buckling in the intermediate range occurs due to mode interaction between the local (flange) and global (Euler) buckling modes rather than between local buckling and yield as in the case of steel columns. Mode interaction has been shown by Arbocz[8] to reduce the buckling load. In this paper, a phenomenological design equation is presented to represent the buckling envelope for pultruded composite I-beams. The formulation accounts for the interaction between local (flange) and global (Euler) buckling modes. In the formulation, an adjustable interaction parameter was used to also account for various material imperfections and interaction levels apparent in pultruded members. The interaction constant is determined through a series of tests described in this paper.

2 STEEL INTERACTION CURVES

Experimental data on steel columns deviate from predictions based on Euler's column buckling formula due to inelastic behavior of the material in the short to intermediate column range. Considère[9] and Engesser[10] developed a theory for inelastic buckling in the short to intermediate column range. The tangent modulus theory states that Euler's formula would be valid if the modulus of elasticity E were replaced by the tangent modulus of elasticity E_t. In this theory, it is assumed that the bending stress distribution due to buckling adds to the uniform compressive stress in the column. Engesser[11] proposed a second theory, the double modulus theory or reduced modulus theory, which states that the modulus of elasticity E in Euler's formula must be replaced by a reduced modulus E_r which is a function of the tangent modulus, the elastic modulus, and the moments of inertia on each side of the neutral axis. In this theory, the tangent modulus E_t should be used on the concave side and the elastic modulus E on the convex side where stresses relax due to bending.

Bleich[12] compares the reduced modulus and tangent modulus theories with experimental results, showing that the experimental loads fall below the critical load predicted by the reduced modulus theory and closer to the tangent modulus theory. Shanley[13] showed that columns start to deflect at a load significantly below the load predicted by the reduced modulus theory. These deflections occur in combination with an increasing axial load. Thus, Shanley concluded that the tensile strain increments caused by the deflection are compensated by the axial shortening of the column. Hence, there is no stress-relaxation anywhere in the cross-section. Shanley goes further to conclude that the maximum load of the column lies somewhere between the tangent modulus load and reduced modulus load.

The tangent and reduced modulus theories can physically explain the inelastic buckling of short and intermediate columns but are rather cumbersome from a design standpoint due to the variability of the tangent modulus with stress. Hence, design of column members is simplified by the use of empirical formulations.

According to the recommendations of the Column Research Council (CRC),[14,15] a single curve is used to model the mean trend of various types of columns. On the CRC curve, the critical stress is plotted against column slenderness. This design curve can be nondimensionalized by plotting σ_{cr}/σ_y against a universal slenderness ratio $\lambda_c = L/\rho(\sigma_y/\pi^2 E)^{1/2}$. The CRC curve is given by

$$\begin{aligned} &\text{For}\,\frac{L}{\rho} < c \quad \sigma_{cr} = \sigma_y\left[1 - \frac{1}{2c^2}\left(\frac{L^2}{\rho^2}\right)\right] \\ &\text{For}\,\frac{L}{\rho} \geq c \quad \sigma_{cr} = \frac{\pi^2 E}{(L/\rho)^2} \end{aligned} \tag{1}$$

where $c = (2\pi^2 E/\sigma_y)^{1/2}$. The equation does not reflect any safety factors or particular restrictions which may be implied by specific design codes.

3 WOOD INTERACTION CURVES

Column design equations for wood members are usually viewed as empirical equations for the compressive strength as a function of slenderness. Zahn[16] develops a column design equation for timber columns by viewing column failure as the interaction between crushing and buckling. In his analysis, Zahn uses the Ylinen[17] equation to model the interaction and develop a universal design equation. Zahn compares the Ylinen column design formulation with other column design equations such as Rankine–Gordon, Perry–Robertson, Neubauer and the fourth-power parabola formulations (reviewed in detail by Zahn[16]). In the Ylinen equation, the parameter c can be viewed as controlling the amount of interaction between crushing and global (Euler) buckling. Zahn states that the parameter c accounts for the effects of nonlinear compression and inhomogeneity of the material. Zahn goes further to state that the parameter c may also be used to automatically include the effect of crookedness as long as the column test specimens are randomly selected from an appropriate sample of columns. Due to its versatility, the Ylinen equation surpasses other empirical equations in which all interaction is assumed to be equivalent to load eccentricity.

The column design equation presented by Zahn is

$$r = \frac{1 + 1/\lambda^2}{2c} - \sqrt{\left(\frac{1 + 1/\lambda^2}{2c}\right)^2 - \frac{1}{c\lambda^2}} \tag{2}$$

where

$$r = \frac{\text{actual strength}}{\text{rupture strength}} \tag{3}$$

and λ is a universal slenderness ratio, independent of material properties, defined as

$$\lambda = \frac{1}{\pi}\frac{L}{\rho}\sqrt{\frac{F_c}{E}} \tag{4}$$

where F_c is the compressive strength. Note that by this definition

$$\lambda^2 = \frac{s}{r} \tag{5}$$

where

$$s = \frac{\text{actual strength}}{\text{buckling strength}} \tag{6}$$

This shows that slenderness is the controlling parameter in the interaction of the two modes.

Note that by the definition of r and s, linear interaction is defined as

$$r + s = 1 \tag{7}$$

Linear interaction is a conservative approximation for design purposes. But using available column data, Zahn points out that the sum of r and s should exceed one. Thus, another term is added to eqn (7). In order to preserve symmetry, the product of r and s is added, and eqn (7) becomes

$$r + s = 1 + crs \tag{8}$$

Equation (8) models linear interaction if $c = 0$ and the noninteraction case if $c = 1$. Interaction between crushing and Euler buckling results in an intermediate value of c to be found experimentally. This equation was presented first by Ylinen[17] and later adopted by Zahn[16] to model wood columns; Zahn also proposed to interpret c as an interaction parameter.

4 PULTRUDED I-BEAM INTERACTION CURVES

Unlike wood and steel, FRPs remain linear for large values of strain. The interaction occurs between local and global modes unless the column is so short that material crushing also occurs. Following the approach of Zahn,[16] a phenomenological column design equation for pultruded I-beams is developed to account for the interaction between the local and global buckling observed in this experimental program. The buckling strength ratios q and s are defined as follows:

$$q = \frac{\text{actual failure load}}{\text{local buckling load}} = \frac{\text{actual strength}}{\text{local buckling strength}} \tag{9}$$

$$s = \frac{\text{actual failure load}}{\text{Euler buckling load}} = \frac{\text{actual strength}}{\text{Euler buckling strength}} \tag{10}$$

Equation (8) can now be applied to represent interaction of local and global modes in FRP columns (note that q replaces r in Zahn's formulation). The controlling parameter c is used to model the amount of interaction between local (flange) buckling and global (Euler) buckling. In the limiting cases, if $c = 0$ linear interaction results, and if $c = 1$ the case of noninteraction is recovered (Fig. 1).

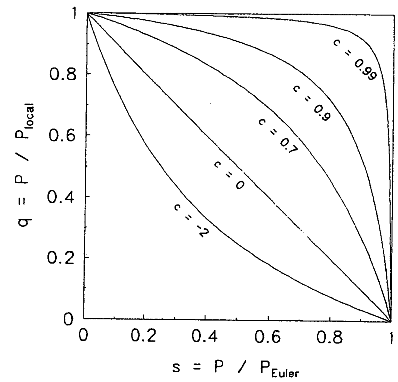

Fig. 1. Various values for the interaction constant c.

A universal slenderness ratio for pultruded I-beam columns can be defined as

$$\lambda = kL\sqrt{\frac{P_{\text{local}}}{D\pi^2}} \tag{11}$$

where k is the effective length coefficient, L is the column length, D is the bending stiffness and P_{local} is the theoretical local buckling load. The effective length coefficient k is given by analytical formulation for columns with various end conditions found in many strength of materials textbooks and design manuals. Since $P_{\text{Euler}} = \pi^2 D/L^2$, using eqn (11) we obtain $P_{\text{Euler}} = P_{\text{local}}/\lambda^2$ which when substituted into eqn (8) gives

$$c\lambda^2 q^2 - (1 + \lambda^2)q + 1 = 0 \tag{12}$$

The root of this equation is

$$q = \frac{P_{\text{cr}}}{P_{\text{local}}} = \frac{1 + 1/\lambda^2}{2c} - \sqrt{\left(\frac{1 + 1/\lambda^2}{2c}\right)^2 - \frac{1}{c\lambda^2}} \tag{13}$$

which represents actual values of q determined experimentally and described by the interaction parameter c with λ given by eqn (11). Therefore, eqn (13) can be used as a design equation over the entire range of column slenderness, short, intermediate, and long. The bending stiffness D of a FRP column is computed from the information provided by the manufacturer for each section following the methodology developed by Barbero[18] for pultruded composite beams. This information includes the type of fibers and matrix material, the local and orientation of the fibers and the fiber content in the cross-section (Fig. 2). Table 1 shows the flange and web bending stiffness components for a 102 mm × 102 mm × 6·4 mm (4″ × 4″ × 1/4″) and 152 mm × 152 mm × 6·4 mm (6″ × 6″ × 1/4″)

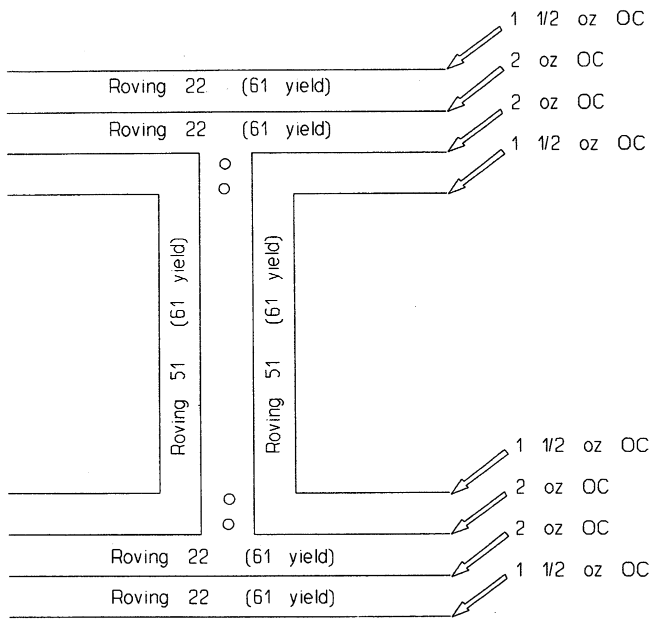

Fig. 2. Creative Pultrusions schematic for the 152 mm × 152 mm × 6·4 mm (6″ × 6″ × 1/4″) WF I-beam.

pultruded WF I-beam, respectively, for bending about the weak axis. The local buckling loads were predicted based on the same information using the analysis presented by Barbero and Raftoyiannis[19]. The maximum interaction between local and global buckling occurs when $q = s$. Using $\lambda = 1$ in eqn (11), the column length for which maximum interaction occurs is

$$L^* = \frac{1}{k}\sqrt{\frac{D\pi^2}{P_{\text{local}}}} \tag{14}$$

TABLE 1

Weak Axis Bending Stiffness Components of the Flanges and Web for Each of the WF I-Beam Sections Tested (note: $D_{16} = D_{26} = 0$ for each section)

Stiffness Component	*102 mm × 102 mm × 6·4 mm*		*152 mm × 152 mm × 6·4 mm*	
	Flanges (M N-cm)	*Web (k N-cm)*	*Flanges (M N-cm)*	*Web (k N-cm)*
D_{11}	13·176	43·720	30·295	46·217
D_{22}	4·958	20·747	11·628	21·052
D_{12}	1·878	8·181	4·435	8·267
D_{66}	1·652	6·603	3·852	6·736

TABLE 2
Maximum Interaction Length L^* for Each Pultruded WF I-Beam Section

Section (mm)	L^* *(cm)*	P_{local} *(kN)*	D *(MN cm²)*
102 × 102 × 6·4	105·9	223·25	253·71
152 × 152 × 6·4	221·5	175·12	872·31

Table 2 shows the value of L^* along with the local buckling load and the weak axis bending stiffness D for each WF I-beam section considered in this paper. L^* corresponds to a length in which maximum interaction between local and global buckling is expected. Therefore, experimental data to obtain the interaction constant should be gathered at this length.

Using the universal slenderness ratio and the ratio of $q = P_{cr}/P_{local}$, the theoretical buckling envelopes for all WF I-beam sections can be collapsed into one universal curve (shaded area in Fig. 3).

5 EXPERIMENTAL RESULTS

The intermediate column tests were performed on the following pultruded WF I-beams: 152 mm × 152 mm × 6·4 mm (6″ × 6″ × 1/4″) and 102 mm × 102 mm × 6·4 mm (4″ × 4″ × 1/4″). More tests were done on

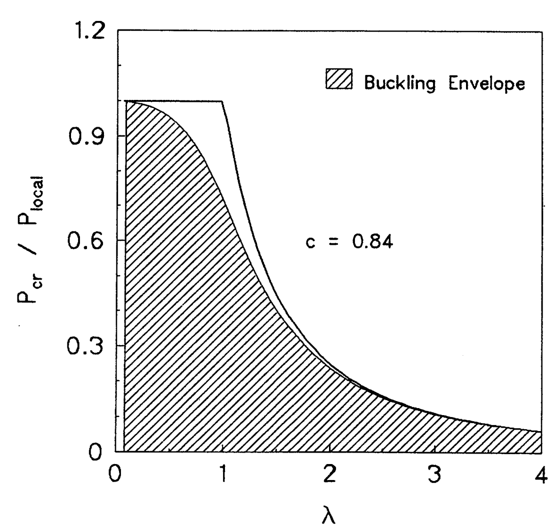

Fig. 3. Buckling envelope accounting for local–global buckling interaction.

the former I-beam because it has a wider range of lengths where interaction occurs. The testing procedure for the intermediate column lengths consisted of loading the specimen with controlled axial displacement. The load, the axial displacement, and the transverse deflection at the midspan were measured by a load cell and two LVDTs. The data was filtered from noise and recorded using a data acquisition system and a moving average technique.[20] The test was continued until the ultimate load of the column was achieved. The ultimate load was also recorded with a peak indicator on the Materials Testing System (MTS) control console. The data reduction simply consisted of obtaining the maximum load the column was capable of supporting, as recorded by the peak indicator on the MTS control console.

Since the span of the intermediate column range had not been previously established, the exact column lengths in the intermediate range were unknown. Hence, the testing lengths were taken between the longest local buckling test available and the shortest Euler buckling test previously performed.[4,21] All tests were conducted with the weak axis of the section in the pinned–pinned configuration. A larger number of samples correspond to lengths close to the predicted L^*. At lengths sufficiently far from L^*, only one test was done.

5.1 152 mm × 152 mm × 6·4 mm (6″ × 6″ × 1/4″) WF I-beam results

Intermediate column tests were performed on the pultruded 152 mm × 152 mm × 6·4 mm (6″ × 6″ × 1/4″) WF I-beam. An increased number of tests were performed around the value of L^* predicted in Table 2. The starting column length was 3·27 m (129″). This length was chosen due to the known Euler behavior apparent when testing a 3·58 m (141″) specimen.[4,21] Hence, column lengths were cut from 3·58 m (141″) progressively shorter in 30·5 cm (12″) increments.

Figure 4 shows the data acquired during the test of a 152 mm × 152 mm × 6·4 mm (6″ × 6″ × 1/4″) WF I-beam (deflection–load plot). Table 3 shows the lengths, theoretical local buckling load, theoretical Euler buckling load and maximum experimental load for each length tested. As seen in Fig. 4, once the maximum load was reached, the lateral deflection increased with decreasing compressive load, indicating a drastic loss of stiffness. As seen from Table 2, a significant decrease in critical load is obtained around the value of L^*. This indicates interaction between the local and global buckling modes. This interaction was also physically apparent during the test in which local flange buckling occurred in combination with lateral deflection. It must be noted that local–global interaction could be observed during the test because of the closely

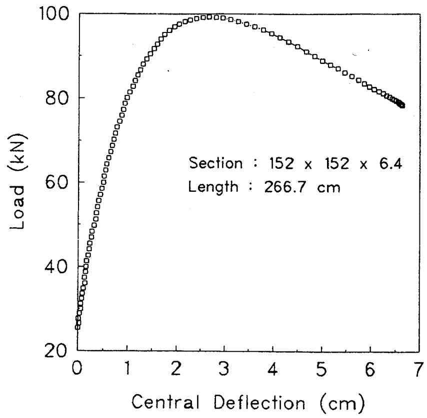

Fig. 4. Experimental intermediate test data on the 152 mm × 152 mm × 6·4 mm (6″ × 6″ × 1/4″) WF I-beam (length = 266·7 cm).

controlled displacement of the column ends obtained by the servo-controlled actuator.

5.2 102 mm × 102 mm × 6·4 mm (4″ × 4″ × 1/4″) WF I-beam results

Intermediate column tests were also performed on the pultruded 102 mm × 102 mm × 6·4 mm (4″ × 4″ × 1/4″) WF I-beam. Since the range

TABLE 3
Experimental Intermediate Test Data on the 152 mm × 152 mm × 6·4 mm (6″ × 6″ × 1/4″) WF I-Beam

Length (cm)	P_{local} *(kN)*	P_{Euler} *(kN)*	$P_{exper.}$ *(kN)*
144·8	175·33	418·00	174·34
175·3	175·33	280·23	148·99
175·3	175·33	280·23	157·23
175·3	175·33	280·23	151·15
175·3	175·33	280·23	156·45
205·7	175·33	203·38	136·83
205·7	175·33	203·38	133·06
205·7	175·33	203·38	138·18
236·2	175·33	152·64	116·67
236·2	175·33	152·64	115·40
236·2	175·33	152·64	120·10
266·7	175·33	121·03	99·23
297·2	175·33	97·48	78·19
327·7	175·33	80·18	67·13

TABLE 4
Experimental Intermediate Test Data on the 102 mm × 102 mm × 6·4 mm (4″ × 4″ × 1/4″) WF I-Beam

Length (cm)	P_{local} *(kN)*	P_{Euler} *(kN)*	$P_{\text{exper.}}$ *(kN)*
114·3	223·52	191·68	171·08
114·3	223·52	191·68	161·98
147·3	223·52	115·39	98·53
147·3	223·52	115·39	95·29
177·8	223·52	79·21	71·58

on intermediate column is narrower than that of the 152 mm × 152 mm × 6·4 mm (6″ × 6″ × 1/4″) WF I-beam (which is apparent from the theoretical curves), only three possible intermediate lengths were compatible with the testing frame. Therefore, only a limited number of tests were performed on this section with lengths closer to L^* (listed in Table 2) for which the maximum interaction between local and global buckling was expected.

Figure 5 shows the data acquired during the test of a 102 mm × 102 mm × 6·4 mm (4″ × 4″ × 1/4″) WF I-beam (deflection–load plot). Table 4 shows the length, theoretical local buckling load and maximum experimental load for each column tested. As seen from Fig. 5, a loss of stiffness is also experienced at the maximum compressive load. As seen from Table 4, a decrease in the experimental load, when compared to theory, is also experienced, indicating interaction between the local and

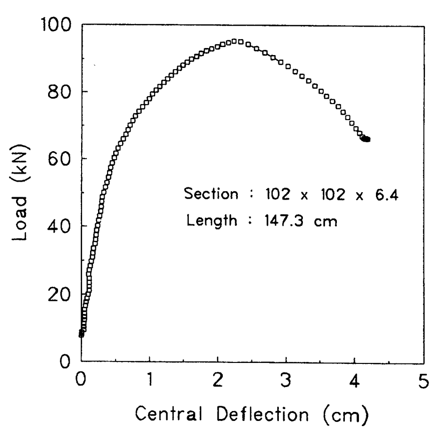

Fig. 5. Experimental intermediate test data on the 102 mm × 102 mm × 6·4 mm (4″ × 4″ × 1/4″) WF I-beam (length = 147·3 cm).

global buckling modes. It was apparent during the test that both local buckling of the flanges and Euler buckling occurred simultaneously. These observations can be made because the test is not as catastrophic as a result of controlling the axial displacement with the hydraulic servo-controlled MTS.

6 DETERMINATION OF INTERACTION CONSTANT

Figure 6 shows the experimental interaction data plotted on an s versus q plot (P/P_{Euler} vs P/P_{local}) for the 152 mm × 152 mm × 6·4 mm (6″ × 6″ × 1/4″) and 102 mm × 102 mm × 6·4 mm (4″ × 4″ × 1/4″) pultruded WF I-beams. As seen from Fig. 6, symmetry appears to exist between the experimental failure loads. Thus, the use of eqn (8) as an interaction equation appears to be valid. Using the data in Tables 3 and 4, the interaction constant c was determined for the pultruded WF I-beam sections. The interaction constant physically describes the degree of interaction present between the local and global buckling failures. For each sample, the value of the interaction constant c was found by solving eqn (8) for c:

$$c = \frac{q + s - 1}{qs} \tag{15}$$

The interaction constant c for each type of cross-section was inferred from the experimental data by averaging the value of c of all samples. For the 152 mm × 152 mm × 6·4 mm (6″ × 6″ × 1/4″) section, an interaction constant of $c = 0{\cdot}85$ was obtained. Similarly, for the 102 mm × 102 mm × 6·4 mm (4″ × 4″ × 1/4″) section, an interaction

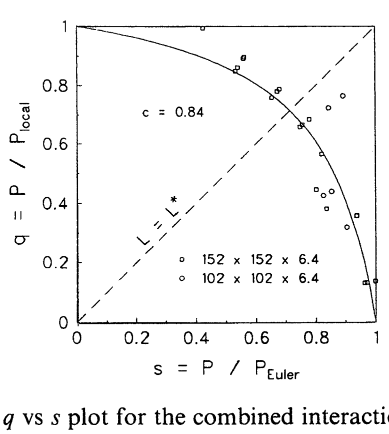

Fig. 6. Nondimensional q vs s plot for the combined interaction test data ($c = 0{\cdot}84$).

constant of $c = 0{\cdot}83$ was obtained. Comparing the values of the interaction constants, it seems that the interaction constant is independent of the size of the cross-section. However, additional I-beam sections should be tested to verify this result. Figure 6 also shows an average interaction constant of $c = 0{\cdot}84$ for both sections tested. As seen from the figure, the value of the interaction constant $c = 0{\cdot}84$ fits the experimental data obtained from the intermediate test.

Using the interaction constant c to approximate the interaction between local and global buckling, an overall buckling envelope is shown by the solid line in Fig. 7. Thus, it is proposed to use eqn (13) as a design equation for the buckling of pultruded composite I-beams. The buckling envelope shown by a solid line in Fig. 7 is valid for any pultruded I-beam section (similar to the sections used in this investigation) provided the values of the bending stiffness D, the local buckling load P_{local} and the interaction constant c are known. Also shown in the figure is additional experimental data obtained by Barbero and Tomblin[4] in the Euler column range. As seen in Fig. 7, the design equation closely approximates the true value of the failure load obtained in experiments.

Interaction is very pronounced for columns with lengths closer to L^*, as seen in the experiments. In this region, column failure occurs and rapidly induces large deformations and material failure (fiber breakage and delaminations). The importance of the interaction curve is evident from a design viewpoint. If the interaction value were not used, a difference of approximately 25% between the theoretically predicted local buckling load and the actual column failure load would be experienced at L^*. Furthermore, the proposed design equation is simpler to use than an Euler equation for long columns and a local buckling equation for short columns.

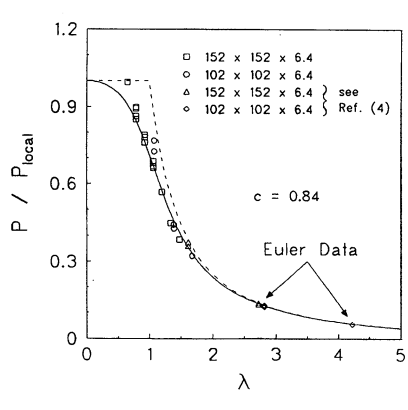

Fig. 7. Nondimensional q vs λ plot with intermediate and global buckling test data.

7 CONCLUSIONS

It is apparent that the design equation presented predicts well the actual critical loads of FRP columns of the type used in this investigation. The value of the interaction parameter $c = 0{\cdot}84$ provides a good estimate of the interaction between local and global buckling for the columns tested. The buckling envelope for pultruded composite WF I-beams shows good correlation with the experimental data developed in this investigation. Although more testing on other WF sections should be done in the future, the interaction curve and design envelope presented provide a basis for the design and use of pultruded structural members in engineering applications. Interaction of local and global buckling modes dominates the intermediate range of lengths of FRP columns used in this investigation. The definition of universal slenderness λ and buckling strength q proposed in this paper lead to a simple design equation to be used for the buckling of FRP columns.

The proposed design equation is based on a phenomenological approach. The interaction constant must be determined experimentally for each new section following the procedure presented in this work. All the sections used in this investigation can be described by the same value of the interaction constant. However, more experimentation is needed to determine if the interaction constant is independent of the cross-section. The validity of the proposed design equation for other types of sections not included in this investigation should be verified by additional experimentation. Development of a theoretical model for buckling mode interaction of FRP columns is underway.

ACKNOWLEDGEMENTS

This research was supported by Creative Pultrusions, Inc. The materials used in this investigation were supplied by the same company. Their collaboration is gratefully acknowledged. The help of the technicians in the College of Engineering at West Virginia University is also appreciated.

REFERENCES

1. GangaRao, H. V. S. & Barbero, E. J., Structural application of composites in construction. In *Encyclopedia on Composites*, ed. S. Lee, VCH Publications, New York, NY, 1991, Vol. 6, pp. 173–87.
2. Ashley, S., Advanced composites take flight. *Mechanical Engineering*, October 1991, 51–6.

3. *Creative Pultrusions Design Guide*. Creative Pultrusions, Inc., Pleasantville Industrial Park, Alum Bank, PA, 1988.
4. Barbero, E. J. & Tomblin, J. S., Euler buckling of thin-walled composite columns. *Thin-Walled Structures*, In Press. (1993).
5. Raftoyiannis, I. G., *Buckling of Pultruded Composite Columns*. MSCE Thesis, Department of Civil Engineering, West Virginia University, WV, 1991.
6. Tomblin, J. S. & Barbero, E. J., Local buckling experiments on FRP columns. *Thin-Walled Structures*, In Press. (1993).
7. Yuan, R. L., Hashen, Z., Green, A. & Bisarnsin, T., Fiber-reinforced plastic composite columns. In *Advanced Composite Materials in Civil Engineering Structures*, ed. S. L. Iyer, ASCE, Las Vegas, NV, 31 January–1 February 1991, pp. 205–11.
8. Arbocz, J., *Buckling and Postbuckling*. Springer-Verlag, Berlin, 1987.
9. Considère, A., Résistance des pièces comprimées. *Congrès International des Procédés de Construction*, Paris, 1891, Vol. 3.
10. Engesser, F., Ueber die Knickfestigkeit gerader Stabe. *Zeitschrift für Architektur und Ingenieurwesen*, Vol. 35, 1889.
11. Engesser, F., Knickgragen. *Schweitzerische Bauzeitung*, Vol. 26, 1895.
12. Bleich, F., *Buckling Strength of Metal Structures*. McGraw-Hill, New York, 1952.
13. Shanley, F.R., Inelastic column theory. *J. Aero. Sci.*, **14**(5) (1947) 261.
14. Galambos, T. V., *Guide to Stability Design Criteria for Metal Structures*, Column Research Council, 4th edn. John Wiley, New York, 1988.
15. Bazant, Z. P. & Cedolin, L., *Stability of Structures*. Oxford University Press, New York, 1991.
16. Zahn, J. J., Re-examination of Ylinen and other column equations, interaction of rupture and buckling in wood members. *ASCE J. Struct. Eng.*, **118**(10) (1992) 2716–28.
17. Ylinen, A., A method for determining the buckling stress and the required cross-sectional area for centrally loaded straight columns in elastic and inelastic range. *Publ. Int. Assoc. Bridge and Structural Engineering*, Zurich, Vol. 16, 1956.
18. Barbero, E. J., Pultruded structural shapes — from the constituents to the structural behavior. *SAMPE J.*, **27**(1) (1991) 25–30.
19. Barbero, E. J. & Raftoyiannis, I. G., Buckling analysis of pultruded composite columns. In *Impact and Buckling of Structures*, ed. D. Hui & I. Elishakoff, ASME, New York, AD-Vol. 20, AMD-Vol. 114, 1990, pp. 47–52.
20. *Labtech Notebook* (version 6). Laboratory Technologies Corporation, Wilmington, MA, 1990.
21. Tomblin, J. S., *A Universal Design Equation for Pultruded Composite Columns*. MSME Thesis, Department of Mechanical and Aerospace Engineering, West Virginia University, WV, 1991.